SUPPLEMENTAL INFORMATION APPENDIX

1. RESULTS

Virus-labeled LGN neurons

Following rabies virus injection into the LGN, multiple neuronal populations were labeled with virus including: corticogeniculate (CG) neurons, retinogeniculate neurons, thalamic reticular nucleus (TRN) neurons, and LGN interneurons. We observed virus-labeled LGN interneurons in most, but not all experimental animals (from a total of 11 experimental animals) and we never observed any virus-labeled neurons in the LGN in 9 control animals in which virus was injected into structures surrounding the LGN. Numbers of virus-labeled LGN interneurons in experimental animals varied from 0-141 (average=22, median=10; **Figs. S1A**-**B**, green dots). Most virus-labeled LGN interneurons (85%) were located within virus injection zones. See **Figure S1B** for photographs of example virus-labeled LGN interneurons located near virus injection zones. Finally, virus-labeled LGN interneurons were more numerous in experimental animals with larger virus injection zone volumes (**Fig. S2A**).

V1 LED-responsive (LEDR) neuronal onset response latencies to LED flashes

Onset response latency following each LED flash was measured for 9 LEDR neurons in 3 experimental animals in order to quantify the latency, time-locking, and temporal jitter in LEDR spiking responses to LED flashes. LED flash onset response latency was calculated as the time to reach 50% of the maximum firing rate following each LED flash. LEDR neurons responded on average 5.7±1.2ms following LED flash onset. Since LED flashes were about 5ms in duration and the variance in LEDR onset response latencies was quite small, these results indicate that LEDR neurons responded in a time-locked fashion to LED flashes with very little temporal jitter. The firing rates of other V1 neurons (non-LEDR) did not increase or decrease relative to spontaneous levels in response to LED flashes (**Figs. 1E**-**F**).

LED-only facilitation of 2 LGN neurons likely due to high CG axonal convergence

Only 2 out of 21 LGN neurons demonstrated a significant increase in response magnitude with LED-only stimulation (**Fig. S2B**, green curves). The majority of LGN neurons were not modulated by LED-only stimulation, showing no increase in firing rates above spontaneous levels (**Fig. 1E**-**F**). LED-only

modulation of 2 LGN neurons was not due to large virus injections or widespread infection as there was a weak negative relationship between virus injection zone volume and LED-only modulation of LGN neurons (**Fig. S2C**). Interestingly, LED-only stimulation generated a short-latency increase in LGN LFP amplitude occurring earlier than the visually evoked LGN LFP peak (**Fig. S2G**). The amplitude of the LED-evoked LFP was small and there was no evidence of longer-lasting changes in LGN LFPs following LED-only stimulation of the cortex (**Fig. S2G**). These results suggest that LED-only modulation of LGN neuronal spiking activity was likely due to high convergence of infected CG axons onto these neurons. Importantly, direct LED stimulation of LGN neurons was highly unlikely because the LED, positioned over the visual cortex, was not powerful enough to penetrate ~7mm into the brain (1). Furthermore, the LED had no impact on LGN activity in control animals in which no CG neurons expressed ChR2 (**Fig. S2E**).

LED stimulation had no impact on LGN or V1 neuronal responses in control animals

LED only stimulation of the visual cortex did not alter the activity of LGN neurons in control animals (p=0.4; n=23 LGN neurons in 9 control animals; LGN control spontaneous firing rate without LED=10.6±1.6 spikes/sec; with LED=10.2±2.7 spikes/sec). LED only stimulation in control animals caused no change in LGN neuronal firing rate above or below the standard deviation of the mean spontaneous firing rate (**Fig. S2E**). Additionally, LED stimulation of the visual cortex did not change firing rates above or below spontaneous levels for 11 V1 neurons recorded in 2 control animals (p=0.2; V1 control spontaneous firing rate without LED=4.8±0.8 spikes/sec; with LED=5.2±0.9 spikes/sec).

LGN neuronal physiology did not differ between control and experimental animals

Because it is likely we recorded from LGN neurons within or near virus injection zones, we tested whether LGN neurons recorded in experimental animals were normally responsive compared to LGN neurons recorded in control animals. To verify that virus infection did not alter the physiology of LGN neurons, we measured spontaneous and visually evoked firing rates for LGN neurons recorded in control (n=22 LGN neurons in 9 animals; average spontaneous firing rate=5.0±0.7 spikes/sec, average vis-

ually evoked firing rate=16.0±1.7 spikes/sec) and experimental animals (n=52 LGN neurons in 9 animals; average spontaneous firing rate=3.7±0.5 spikes/sec, average visually evoked firing rate=19.3±2.3 spikes/sec). We observed no significant differences in either spontaneous or visually evoked firing rates across LGN neurons recorded in control and experimental animals (p>0.1 for both). We also observed no differences in our hit rates for recording visually responsive LGN neurons in control and experimental animals (2.9 LGN neurons recorded per array penetration in 9 experimental animals; 2.4 LGN neurons recorded per array penetration in 9 control animals).

V1 neuronal physiology did not differ between control and experimental animals

To confirm that virus infection did not alter the physiology of CG neurons, we measured spontaneous and visually evoked firing rates for V1 LEDR neurons (n=9 LEDR neurons in 3 experimental animals; LEDR: average spontaneous firing rate=8.9±3.2 spikes/sec, average maximum visually evoked firing rate=15.0±3.9 spikes/sec), V1 non-LEDR neurons (n=17 non-LEDR neurons in 3 experimental animals; non-LEDR: average spontaneous firing rate=8.9±2.5 spikes/sec, average maximum visually evoked firing rate=17.9±3.6 spikes/sec) and V1 neurons recorded on deep layer contacts in control animals (n=13 deep layer neurons in 2 control animals; V1 deep layer control: average spontaneous firing rate=4.8±0.3 spikes/sec, average maximum visually evoked firing rate=13.5±1.8 spikes/sec). We observed no significant differences in either spontaneous or visually evoked firing rates across these three V1 neuronal subpopulations (p>0.6 for both).

LED stimulation did not cause long-term saturation or suppression of LEDR neurons

In 3 experimental animals, we measured the average firing rate of V1 LEDR neurons in response to drifting grating stimulation with and without flashed LED stimulation (n=6 LEDR neurons) and in response to m-sequence stimulation with and without continuous LED stimulation (n=10 LEDR neurons). LEDR neuronal firing rates increased by 11.6% for grating+LED stimulation and by 28.5% for m-sequence+LED stimulation compared to visual stimulation alone. These measurements indicate that flashed and continuous LED stimulation increased the overall firing rate of LEDR neurons, but neither

SUPPLEMENTAL INFORMATION APPENDIX

LED stimulation pattern caused saturation or suppression of neuronal firing rates over time (**Fig. S3**). To further quantify whether different LED stimulation patterns caused long-term saturation or suppression of LEDR neuronal activity, we calculated the rate of change of neuronal firing rate over time, as the derivative of firing rate measured across 10ms windows, in response to drifting grating+LED stimulation, phase-reversing grating+LED stimulation, and m-sequence+LED stimulation for 14 LEDR neurons. We found no differences in the rate of change of LEDR firing rates over time across the different patterns and durations of LED stimulation (p=0.6), suggesting that continuous LED stimulation had a similar effect on LEDR neuronal activity as flashed LED stimulation. Importantly, we also examined the rate of change of firing rate for LEDR neurons in response to m-sequence stimulation alone compared to m-sequence stimulation plus LED stimulation and we found no difference (p=0.7), indicating that LEDR neurons were primarily driven by the m-sequence stimulus and continuous LED illumination paired with m-sequence visual stimulation merely increased overall neuronal responsiveness. It is also important to reemphasize that non-LEDR neurons within close proximity to LEDR neurons (within 147μm on average of LEDR neurons), did not respond above or below spontaneous levels to LED stimulation (see **Figs. 1E**-**F**, **S2B**).

CG-mediated reduction in LGN response latency not due to contrast-dependent phase advance, temporal phase advance, or changes in brain state

In some respects, the CG-mediated reduction in LGN onset response latency was reminiscent of contrast-dependent phase advance (2). To test whether the reduction in onset response latency we observed with LED stimulation of CG feedback was consistent with a contrast-dependent phase advance mechanism, we compared the latencies and spike timing precision values of visually evoked LGN neuronal responses to low- and high-contrast gratings without LED stimulation. We observed a small, non-significant reduction in LGN response latency for high-contrast stimuli (p=0.89, n=43; average low-contrast latency=44.2±8ms, average high-contrast latency=42.7±8.3ms) and a small, non-significant increase in response precision for high-contrast stimuli (p=0.12, n=39; average low-contrast standard deviation of spike time=25.7±3.1ms, average high-contrast standard deviation of spike

time=21.4±2.9ms). As these values do not approach the larger latency shifts and increases in response precision observed with LED stimulation of CG feedback (see **Table 1B** and **Fig. 3**), the CG-mediated effects we observed cannot be explained by a contrast-dependent phase advance mechanism alone.

It is also possible that temporal phase advance of LGN neuronal responses could explain the reduction in LGN onset response latency. To test whether LED stimulation led to temporal phase advance among 28 LGN neurons, we calculated the y-intercept of the linear fit to the phase of the F1 response component at increasing grating temporal frequencies. Both with and without LED stimulation, y-intercepts were not different than zero (average y-intercept with LED=0.7±0.7 radians; average y-intercept without LED=-0.04±0.5 radians), nor were y-intercepts different across LED conditions (p=0.14), suggesting that the LED did not cause systematic temporal phase shifts in LGN responses.

To test whether LED stimulation of the visual cortex caused changes in brain state, we examined power in the EEG measured during m-sequence presentation with and without LED stimulation. For 12 recording sessions in 4 experimental animals, we observed no significant differences in EEG power in any frequency band across LED conditions (**Fig. S4**). When we performed a cumulative distribution test on average power spectra, we observed no significant differences across LED conditions (p=0.95). These results suggest that LED stimulation of the visual cortex did not alter brain state.

Increasing LED flash rate explains increase in LGN response magnitude to gratings varying in temporal frequency

We sought to understand why LGN neurons displayed increased maximum firing rate and response magnitude during temporal frequency tuning tests but not contrast and spatial frequency tuning tests. Specifically, we performed two analyses to explore whether different LED stimulation patterns could account for this discrepancy. During contrast and spatial frequency tuning tests, LED flashes were fixed at ~4Hz, in synch with the fixed temporal frequency of those gratings. During temporal frequency tuning tests, the LED flashed at progressively increasing temporal frequencies, again in synch with the increasing temporal frequencies of the gratings. In the first analysis, we compared predicted with actual responses for 12 LGN neurons. For each neuron, the predicted response was the sum of the response

to the visual stimulus alone and the response to LED stimulation alone. The actual response was the response of the same neuron to the visual stimulus paired with LED stimulation. Importantly, for calculations of predicted responses in contrast and spatial frequency tests, neuronal responses to LED only stimulation at 4Hz were used. For calculations of predicted responses in temporal frequency tests, neuronal responses to LED stimulation at increasing flash frequencies were used (e.g. curves illustrated in **Figs. 1E**, **S2B**). Errors between predicted and actual tuning curves were equivalent for all three tuning tests, suggesting that increasing LED flash frequencies utilized for temporal frequency tuning tests contributed to the greater influence of LED stimulation on LGN neuronal responses to stimuli varying in temporal frequency.

As a second test of LGN responses to different patterns of LED stimulation, we decoupled LED flash frequency from visual stimulus temporal frequency. For a subset of LGN neuronal recordings (n=20 in 2 experimental animals), we measured temporal frequency tuning in four conditions: 1) visual stimulus alone; 2) visual stimulus plus LED flashes at the frequency of the visual stimulus; 3) visual stimulus plus LED flashes fixed at 4Hz on all trials; and 4) visual stimulus plus LED flashes at twice the frequency of the visual stimulus. We calculated the maximum firing rate (at the preferred temporal frequency) and response magnitude and compared these across the four conditions listed above. We observed an increase in maximum firing rate and response magnitude compared to no LED stimulation for all LED stimulation patterns. Specifically, LGN responses were minimally increased with fixed 4Hz LED flashes (5% increase on average), further increased with LED flashes coupled to the grating cycle (13% increase on average), and most increased with LED flashes at twice the grating cycle (15% increase on average). However, there were no significant differences in maximum firing rate or response magnitude for these three LED stimulation patterns (p>0.5 for both). Therefore, although we observed no significant differences in maximum visually evoked firing rate or magnitude across different LED flash patterns, there was a progressive increase in LGN activity with higher LED flash rates. Together, these findings suggest that discrepancies in LED modulation of LGN neurons across tuning tests can be explained by higher LED flash rates during temporal frequency tuning tests.
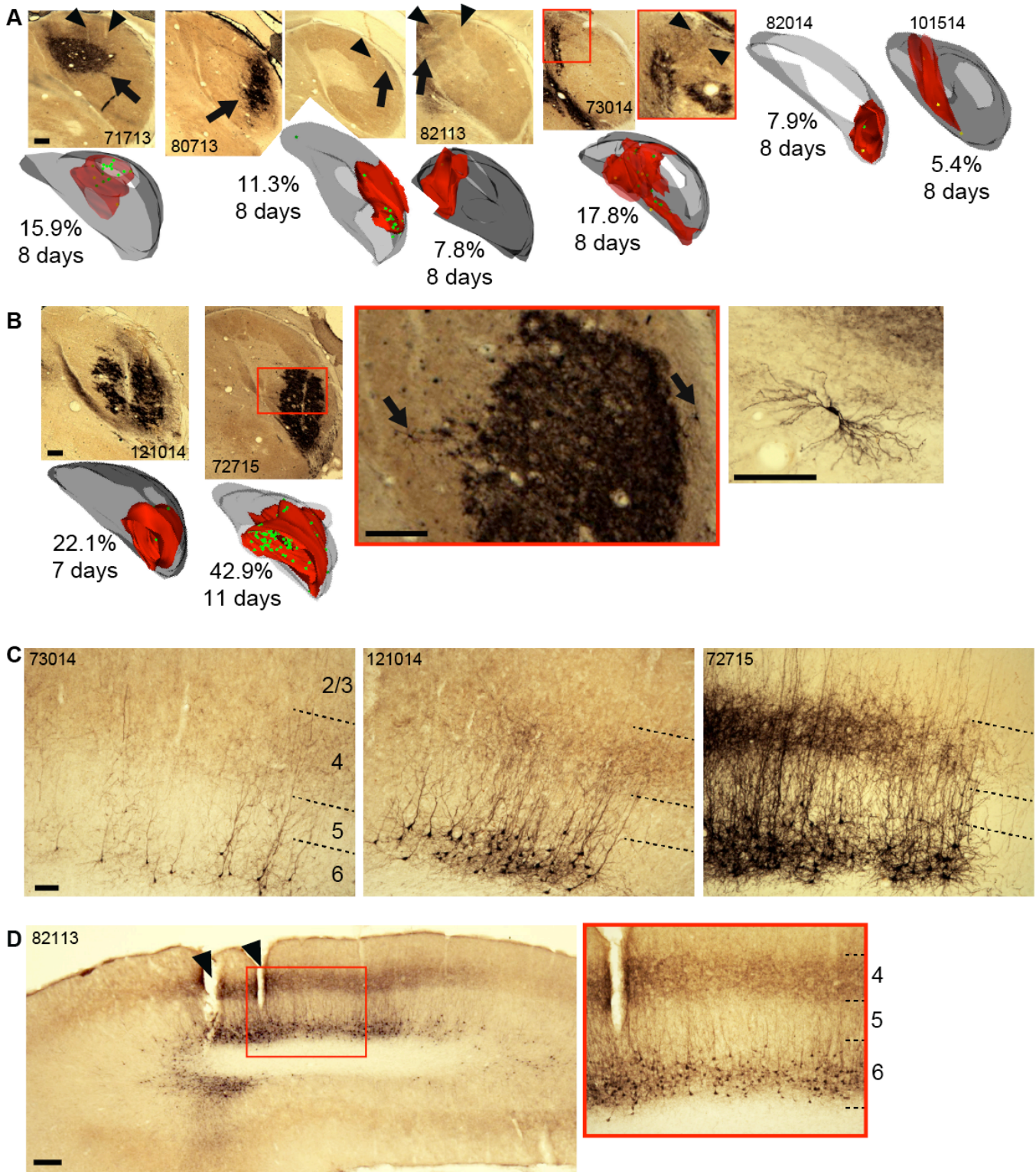
2. FIGURES

Supplemental Figure 1: Virus injection zones, recording electrode track lesions, and virus-labeled neurons in the LGN and in V1.

(A) Photographs and 3-d renderings of virus injection zones in the 6 experimental animals (numerically labeled) from which LGN physiological data were analyzed. Photographs are individual coronal sec-

7

SUPPLEMENTAL INFORMATION APPENDIX

tions through LGNs, dorsal is up, medial is left, and scale bar (in leftmost image) represents 375μm for all examples. Two sections within 200μm of each other are illustrated for animal "80713", the left section illustrates the largest extent of the virus injection zone and the right section illustrates a nearby recording electrode track lesion. Red box in section from animal "73014" outlines higher magnification view illustrated to the right (outlined in red). Arrowheads point to recording electrode track lesions, which are often in parallel due to the arrangement of the 7-channel multi-electrode array. Arrows point to virus injection zones. 3-d renderings of LGNs for each experimental animal illustrate LGN contours (grey) surrounding virus injection zone contours (red). Green dots, mostly within virus injection zone volumes, mark locations of virus-labeled LGN interneurons. Numbers indicate total injection zone volumes as percentages of total LGN volumes and wait times between virus injections and neurophysiological recordings.

(B) Photographs and 3-d renderings of virus injection zones in the 2 experimental animals (numerically labeled) used for anatomical analyses only. Conventions as in (A) and scale bar represents 375μm for both LGN examples. Red box in section from animal "72715" outlines higher magnification view illustrated to the right (outlined in red), illustrating the locations of two virus-labeled LGN interneurons near the virus injection zone (marked by arrows). Scale bar represents 375μm. Rightmost photograph is a higher magnification view illustrating a virus-labeled LGN interneuron, scale bar here represents 190μm.

(C) Coronal sections through V1 (area 17) from 3 experimental animals (numerically labeled). Scale bar in leftmost image represents 250μm and applies to all three images. Layers are indicated by dashed lines and labeled in leftmost image. Note a lack of labeled axons in the white matter or in layer 4, even in denser patches of labeled CG neurons.

(D) Left: wider view of coronal V1 section illustrating patchy distribution of virus-infected CG neurons in layer 6. Recording electrode lesions indicated by arrowheads. Scale bar represents 500μm. Red box outlines image area illustrated at higher magnification to the right (outlined in red) with layers labeled as in C. Note the lack of labeled axons in the white matter or in layer 4, which is darkened due to the cytochrome oxidase stain.
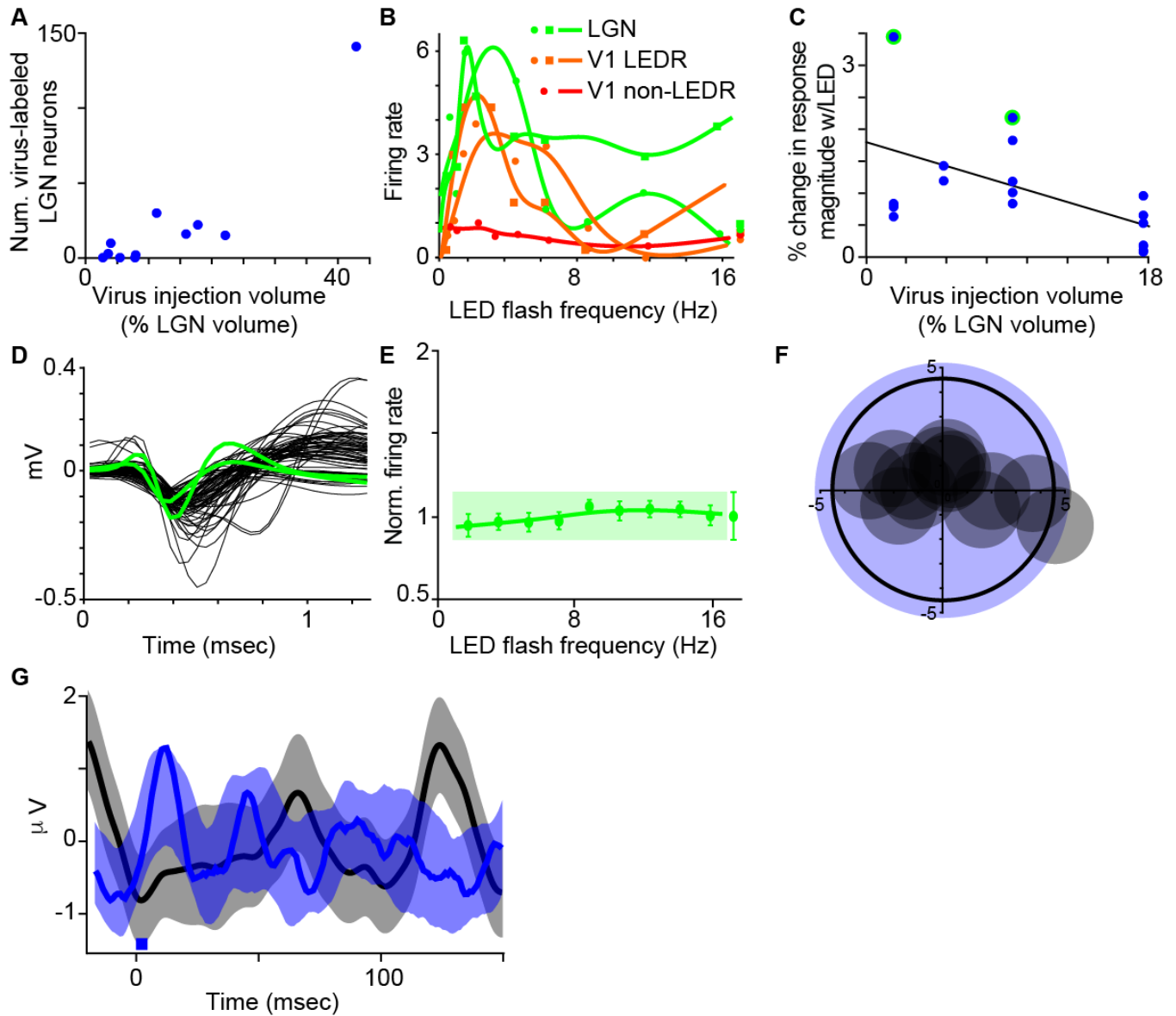
Supplemental Figure 2: LGN neuronal properties.
(A) Relationship between virus injection zone volume (as a percentage of total LGN volume) and the number of virus-labeled LGN interneurons for 11 experimental animals. No virus-labeled neurons were observed in the LGN in 9 control animals. Low numbers of virus-labeled LGN neurons were observed in most experimental animals although larger injection zones correlated with greater numbers of virus-labeled neurons. 85% of virus-infected LGN interneurons were located within virus injection zones.
(B) Example responses of two V1 LEDR neurons (orange), a neighboring, V1 non-LEDR neuron within 200μm of simultaneously recorded LEDR neurons (red), and two LGN neurons (green) to LED-only stimulation at increasing flash frequencies. Responses are normalized to spontaneous activity for each neuron, indicated to the right of the curves. Data are dots; lines are curve fits. Conventions as in **Fig. 1E**.
(C) Comparison of LED-only stimulation of LGN neuronal activity (% change in response magnitude, as in **Fig. 1F**) with virus injection zone volume for 21 LGN neurons recorded in 4 experimental animals. A linear fit to the data revealed a weak negative relationship between total virus injection zone volume and LED-only modulation of LGN neuronal activity (R^2=0.21). The two LGN neurons encircled in green are the only two LGN neurons that were significantly modulated by LED-only stimulation illustrated in B.
(D) Spike waveforms of 68 LGN neurons recorded in 9 experimental animals. The two waveforms high-

SUPPLEMENTAL INFORMATION APPENDIX

lighted in green are the two LGN neurons illustrated B and C that were directly modulated by LED-only stimulation of the visual cortex. Note that almost all waveforms are consistent with regular spiking waveforms in duration and amplitude; and the two green waveforms are similar to the remaining waveforms.

(E) Average responses of 23 LGN neurons (green dots) from 9 control animals (in which no virus was injected into the LGN) to LED stimulation of the visual cortex. Responses are normalized to spontaneous activity levels, illustrated by the green dot to the right. Error bars represent SEMs; curve fit is a smoothing spline. Axes are comparable to those in **Fig. 1E**. Note that all LGN neuronal responses are within the standard error range of spontaneous activity, illustrated by the light green box.

(F) Representation of relative receptive field position of LGN and V1 neurons simultaneously recorded in 13 separate sessions. Black circle illustrates average V1 receptive field with a diameter of 9 degrees, typical for the eccentricities we recorded in ferret area 17 (3, 4). Grey circles illustrate LGN neurons offset from (0,0) by the difference in receptive field center position relative to simultaneously recorded V1 neurons. LGN receptive fields ranged 1-6 degrees so are illustrated as 3 degrees in diameter. Blue circle illustrates the cone of LED illumination in visual degrees according to a ferret V1 magnification factor of 0.2 mm/degree for eccentricities < 20 degrees (5, 6). Thus, the LED stimulation zone was approximately the size of an average V1 receptive field.

(G) Comparison of local field potentials (LFPs) recorded from 7 LGN contacts during 12 experimental sessions (across 4 experimental animals) in response to LED-only stimulation of the visual cortex (no visual stimulation) in blue and gratings (no LED stimulation) in black. Solid lines illustrate average LFPs and shaded regions represent SEMs. Time zero represents LED flash onset (blue box) or grating onset. Note that LFPs in response to LED onset demonstrate a shorter-latency increase in amplitude compared to LFPs in response to grating stimuli. Short-latency LED-evoked responses are consistent with LED-activation of CG neurons. Visual responses emerging around 50ms following visual stimulus onset are consistent with visual response latencies in the LGN. Note also that the amplitude of visually-evoked LFPs are larger than those of LED-evoked LFPs. Furthermore, LED-evoked LFPs do not show any sign of longer-term saturation or suppression.
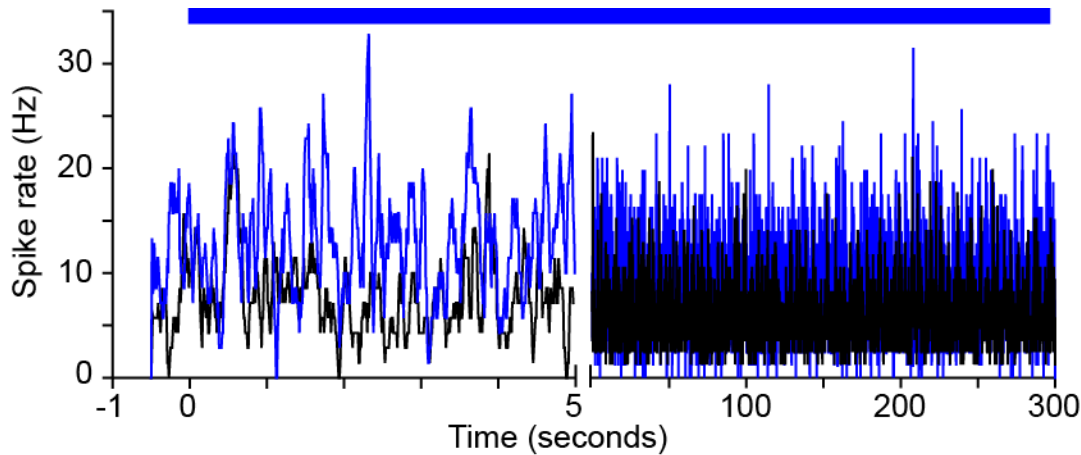
Supplemental Figure 3: V1 neuronal responses during m-sequence stimulation with and without continuous LED illumination.
Average responses of 10 putative V1 CG (LEDR) neurons (recorded in 4 experimental animals) in response to m-sequence visual stimulation alone (black) and in response to m-sequence visual stimulation plus continuous LED illumination of the visual cortex (blue). Time zero represents the onset of the m-sequence and also the onset of LED stimulation (indicated by the blue bar above the curves). Note the change in time scale mid-way along the x-axis. Responses of LEDR neurons were similar prior to the onset of visual or visual + LED stimulation (before time zero). Immediately after the onset of the visual stimulus (or visual + LED stimulation), responses were also similar across conditions. After about 1 second of visual + LED stimulation, the magnitude of LEDR neuronal responses increased with LED stimulation and this small elevation in response magnitude persisted for hundreds of seconds without any indication of saturation or suppression of LEDR neuronal activity with continuous LED illumination. Interestingly, the variance of LEDR neuronal responses appears qualitatively to be slightly increased with LED stimulation. However, overall response patterns were similar across conditions with and without LED stimulation, suggesting that the main driver of LEDR responses was the visual stimulus (m-sequence) and continuous LED illumination caused a small increase in response magnitude without altering visually evoked response patterns.
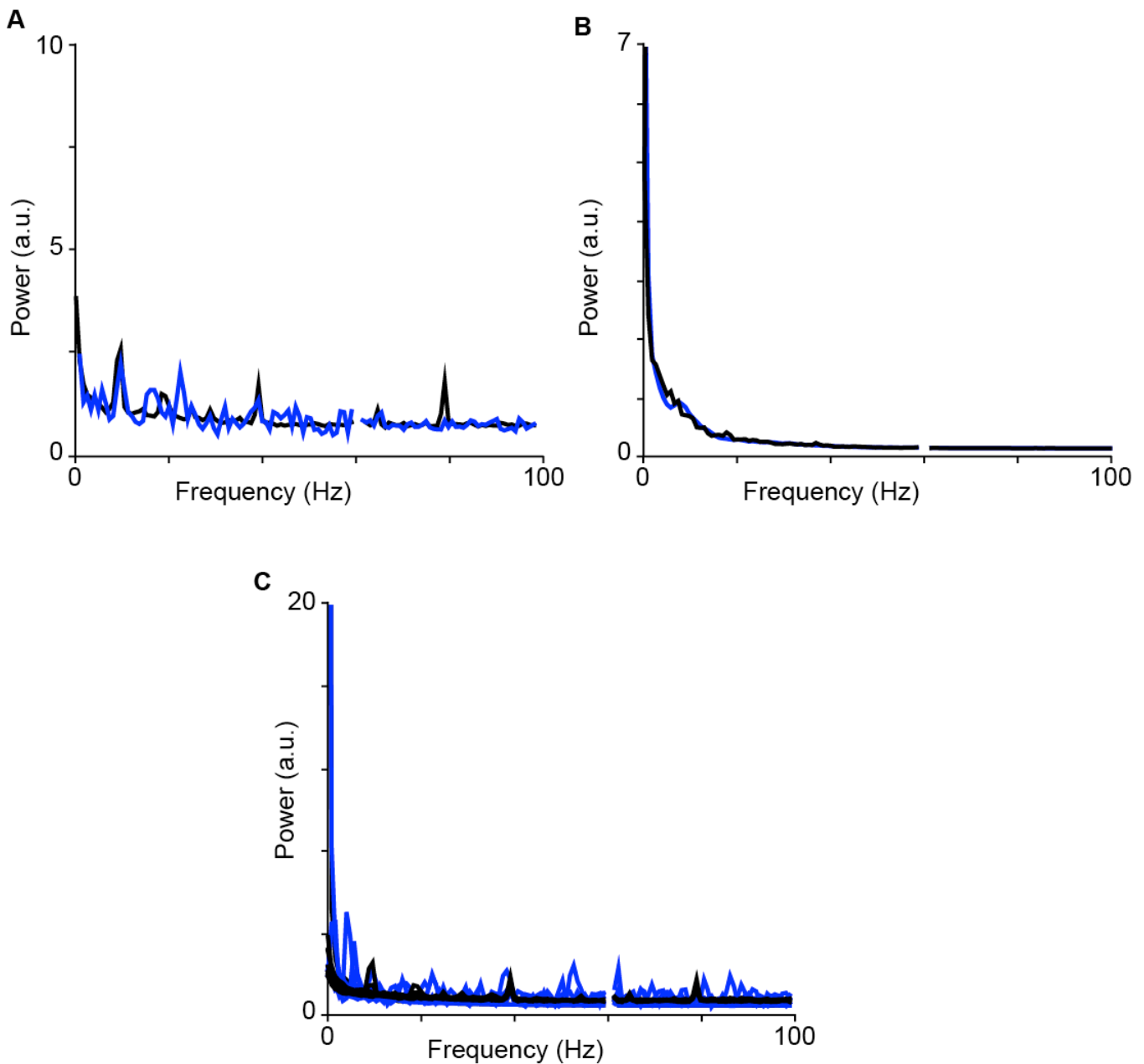
Supplemental Figure 4: EEG power across LED conditions.
(A, B) Two individual session examples from two different experimental animals of EEG power measured during m-sequence visual stimulation with (blue) and without (black) LED stimulation. EEG data were differential voltage signals recorded between two electrodes placed above left and right frontal cortex (continuous data digitized at 8000Hz, low-pass filtered at 200Hz, and down-sampled to 1000Hz). Power spectra were computed by creating rate histograms of voltage data, passing these through a Hann window, applying a Fast Fourier Transform, and extracting amplitudes for frequencies between 1 and 100Hz. Spectra were normalized by the mean squared value of the rate histogram. Data analyses were performed on 10-minute duration segments from the middle of each experimental session (with and without LED stimulation). Values between 59-61Hz represent line noise and have been removed. (C) All power spectra from 12 sessions (recorded across 4 experimental animals). Conventions as in A&B. For statistical comparisons of power spectra across LED conditions, t-tests were performed for frequency analysis windows with widths of 10Hz, using Bonferroni correction for multiple comparisons and a significance criterion of $p < 0.05$. We observed no significant differences in power in any frequency

SUPPLEMENTAL INFORMATION APPENDIX

band between 1 and 100Hz. When we performed a cumulative distribution test on average power spectra, we observed no significant differences across LED conditions (p=0.95). Together, power spectral data show that LED stimulation did not alter brain state. Therefore, the effects we observed of LED stimulation of CG feedback on the response timing and precision of LGN neurons cannot be attributed to LED-induced changes in brain state.
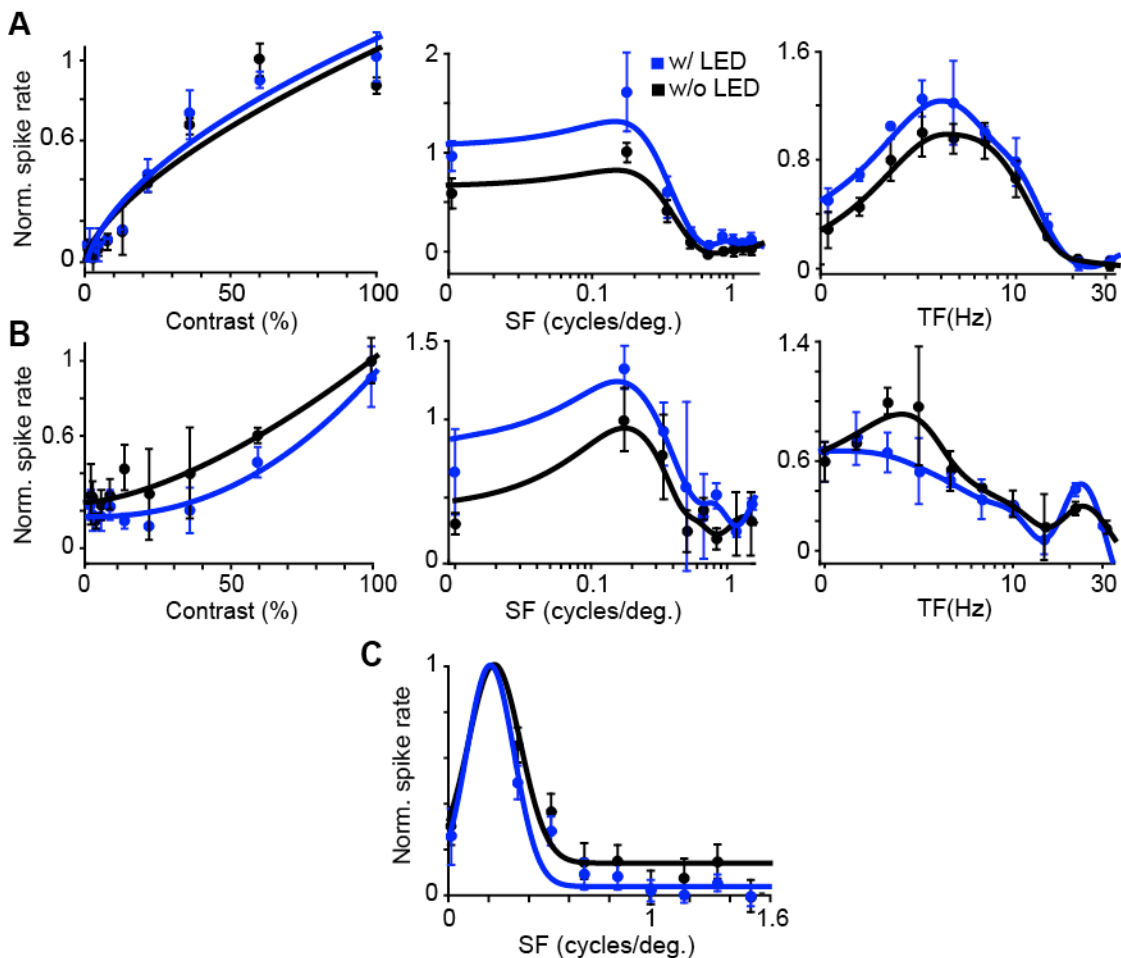
Supplemental Figure 5: Representative LGN tuning curves with and without LED stimulation of CG feedback

Contrast, spatial frequency, and temporal frequency response curve fits for two representative neurons, an LGN Y neuron (A) and an X neuron (B), with (blue) and without (black) LED stimulation of CG feed-back. For each neuron and each response curve, data (dots) are normalized to the peak of the without LED response. Error bars represent SEMs.

(C) Spatial frequency tuning curves plotted on a linear scale, as in (7), for 27 LGN X and Y neurons with (blue) and without (black) LED stimulation of CG feedback. Data (dots) are normalized to the peak to facilitation comparison of curve shapes. Error bars represent SEMs. The full widths of the SF peaks, measured from Gaussian fits (curves) were on average 2.3 octaves with LED stimulation and 3 octaves without LED stimulation. Also note the with-LED stimulation curve (blue) is narrower for higher spatial frequencies, supporting the hypothesis that LED stimulation of CG feedback causes adjustment in the contributions of receptive field subunits to spatial summation within the receptive field (7).

3. MATERIALS AND METHODS

Virus injection

All surgical procedures were conducted in a sterile surgical suite using aseptic techniques. Anesthesia was induced with ketamine (30mg/kg, IM) alone or with xylazine (1mg/kg, IM). Ferrets were then intubated and anesthetic depth was maintained with inhaled isoflurane (1-2.5%). Ferrets were then placed in a stereotax, wrapped in a thermostatically controlled blanket, and prepped for surgery. During surgery, heart rate, respiration rate, $ETCO_2$, SPO_2, and temperature were continuously monitored. A 3cm midline incision was made in the scalp and the temporalis muscles were retracted to reveal the skull. An $8mm^2$ craniotomy was made centered over the stereotaxic coordinates of the LGN (~AP=-1, ML=5.8). A sharp platinum-iridium electrode (FHC, Bowdoin, ME) was inserted through the dura and advanced to the LGN where visual responses to light flashes were confirmed. Injections were targeted to the central visual field region (0-20 degrees) and included A/A1 and/or C layers of the LGN. Following confirmation of LGN location and depth (~7mm), the metal electrode was removed and a glass pipette containing $5\mu l$ of SADΔG-ChR2-mCherry was inserted at the same location. Virus was injected at several depths along the penetration using a pneumatic nanoliter injector (Nanoject II, Drummod Scientific, Broomall, PA). Following injection of the virus and removal of the pipette, the craniotomy was covered with bone wax and the muscles and scalp were sutured closed. Ferrets were given ketoprofen (4mg/kg, IM) for analgesia and baytril (5mg/kg, IM) as an antibiotic and allowed to recover for 7 to 11 days in order to allow for adequate expression of optogenetic proteins in infected corticogeniculate (CG) neurons (8, 9).

Experimental preparation

The neurophysiological recording experiment took place 7 to 11 days following the surgery. Anesthesia induction and surgical preparations were as described above. Instead of intubation, ferrets underwent a tracheotomy and were ventilated with 1-2% isoflurane and a 2:1 mixture of oxygen and nitrous oxide. Throughout the experiment, heart rate, respiration rate, $ETCO_2$, SPO_2, and temperature were continuously monitored and animals received continuous infusion of lactated ringers with dextrose (3ml/kg/hr,

IP) to prevent dehydration. The scalp incision was reopened and the craniotomy extended to expose visual cortex. Small amounts of cerebrospinal fluid (300-500μL) were removed via cisternal puncture and the dura was removed from the area of the craniotomy. Agar in saline (1%) was used to cover the exposed cortex and prevent drying. Subcranial EEG was also measured to monitor anesthetic depth and brain state. Spectral analysis of the EEG revealed that animals were consistently maintained in a stable anesthetic plane. Following all surgical manipulations and a 30-minute physiological monitoring phase, animals were paralyzed with vecuronium or rocuronium bromide (1mg/kg/hr, IP) in order to eliminate eye movements.

Visual stimuli

Grey-scale drifting sinusoidal gratings, phase-reversing gratings, and white noise m-sequence stimuli were presented on a gamma-calibrated CRT monitor (ViewSonic, Brea, CA) with a refresh rate of 100Hz placed at a distance of 45-60cm from animals' eyes. Stimuli were generated with the ViSaGe stimulus generation system (Cambridge Research Systems, Rochester, UK) following custom-written Matlab (Mathworks, Natick, MA) command scripts. Grating stimuli were presented for two seconds followed by two seconds of mean grey. Gratings were between 8 and 20 degrees in diameter such that a single grating overlapped all simultaneously recorded neurons. Alternatively, smaller gratings (4-8 degrees in diameter) were used to record from different groups of neurons. Gratings varied in contrast (0-100%), temporal frequency (1-32Hz), spatial frequency (0.1-2.5 cycles/degree), or orientation (0-324 degrees) in steps of 10. When not varying, grating parameters were fixed at the preferred spatial and temporal frequencies of the majority of recorded LGN neurons, preferred orientation of recorded V1 neurons, and a contrast of 70%. All grating stimuli were displayed 4 times, twice with LED stimulation (see below) and twice without LED stimulation of CG feedback. M-sequence stimuli were 8-25 degrees on each side of a square 24x24 pixel grid and were displayed for 10-20 minutes on each of two repeats, once with and once without LED stimulation of CG feedback. The luminance of each pixel (black or white) modulated according to the m-sequence every two frames. In all cases, visual stimuli were positioned to optimally activate the largest possible number of recorded neurons.

SUPPLEMENTAL INFORMATION APPENDIX

Neurophysiological recordings and preliminary data analyses

Extracellular spikes and local field potentials (LFPs) were recorded from electrode contacts in the LGN and in V1 in response to visual stimuli and LED stimulation of CG feedback. V1 neurons were recorded with a 24-contact linear multi-electrode array (U-Probe from Plexon Inc., Dallas, TX) inserted perpendicular to the cortical surface such that the electrodes spanned all 6 cortical layers within a single column. LGN neurons were recorded with an array of seven independently movable platinum-tungsten microelectrodes (Eckhorn Matrix from Thomas Recording GMBH, Giessen, Germany). Receptive fields of all recorded neurons were mapped using standard hand- and software-assisted mapping procedures. V1 and LGN arrays were placed within retinotopically-aligned regions of the visual cortex and LGN (average receptive field center overlap between V1 and LGN = 90% for 13 sessions, **Fig. S2F**). Signals from both multi-electrode arrays are amplified and duplicated such that high-pass filtered spikes as well as low-pass filtered LFPs were acquired from all channels using an Omniplex data acquisition system (Plexon Inc., Dallas, TX). The laminar positions of V1 recording contacts were determined from current-source density (CSD) profiles generated from visually evoked LFP responses recorded from contacts spanning the cortical depth of V1. The border between layers 4 and 5 corresponds to the first polarity reversal in visually evoked LFPs and CSDs (10). We used this border to identify V1 neurons in the deep layers (one of the criteria for identification of putative CG neurons, see below) and in the granular layers (for **Figs. 3E**-**F**). Similar CSD profiles were generated from V1 LFP responses to LED-only stimulation (see below for LED-only stimulation parameters) in order to determine the laminar location and timing of LED-evoked responses in V1 (**Fig. 1D**). Single unit spikes recorded on all channels were sorted offline using commercial spike sorting software (Plexon Inc., Dallas, TX) employing principal components analysis. Calculations of the signal-to-noise ratios (SNRs) for all sorted spike waveform shapes were made in order to select well-isolated spikes (11) using a cutoff of SNR > 2.75. In order to distinguish putative excitatory (LGN relay neurons) versus inhibitory (LGN interneurons) neurons in the LGN based on spike waveform shape (see **Fig. S2D**), we calculated the peak-to-trough time and the full amplitude (absolute value of the minimum to maximum height) and we compared these values for each LGN neurons in our sample. Only 4 LGN neurons had peak-to-trough time and amplitude values

SUPPLEMENTAL INFORMATION APPENDIX

consistent with putative inhibitory neurons while the remaining 64 LGN neurons had values consistent with excitatory neurons (12).

We defined putative V1 CG neurons based on the following three criteria: 1) single units had to be well-isolated and recorded on linear array contacts that were at least 3 contacts below (>200μm below) the border between layer 4 and layer 5 defined by CSD spectra measured from visually evoked LFP responses (e.g. in **Fig. 1D**) – in other words putative V1 CG neurons had to be located in layer 6; 2) LFPs recorded from the same contacts as putative V1 CG neurons (deep layer contacts as defined by criterion 1, above) needed to show LED-only evoked responses that were time-locked to the LED flash (e.g. in **Fig. 1D**); and 3) each putative V1 CG neuron had to respond to LED-only stimulation with an increase in firing rate greater than 2 standard deviations of its mean spontaneous firing rate (see representative examples in **Fig. S2B**; see below for LED-only stimulation parameters and additional details on analyses of neuronal responses to LED-only stimulation). We calculated our "hit rate" of recording putative V1 CG neurons as the number of well-isolated single units we recorded on deep layer contacts for recording sessions in which the linear array was inserted into a patch of labeled CG neurons. In order to quantify the onset latency, time-locking, and temporal jitter in putative CG spiking responses to LED flashes, we calculated the average onset response latency following LED flash onset for 9 putative CG neurons as the time to reach 50% of the maximum firing rate following each LED flash onset. We also measured peri-stimulus time histograms (PSTHs) for putative CG neurons and other neighboring V1 neurons in response to LED-only stimulation (**Fig. 1C**). Even though putative CG neurons responded rapidly (within 6ms of LED flash onset) and reliably to LED flashes, it is possible that some putative CG neurons in the sample were poly-synaptically activated V1 neurons. We therefore labeled putative CG neurons as LED-responsive or LEDR neurons. Any V1 single unit that did not meet these three criteria was designated as a V1 non-LEDR neuron and those V1 non-LEDR neurons located on linear array contacts in close proximity to LEDR neurons were further identified as "neighboring" V1 non-LEDR neurons.

To verify that virus infection did not alter the physiology of LGN, V1 LEDR, or V1 non-LEDR neurons, we calculated spontaneous and maximum visually evoked firing rates for neurons in these

subpopulations recorded in both experimental and control animals. Additionally, we compared spontaneous firing rates to firing rate modulations with LED-only stimulation for these same subpopulations recorded in experimental and control animals to confirm that LED-only stimulation only altered the activity of neurons in experimental but not control animals. Results of these analyses are reported in Supplemental Results.

Optogenetic stimulation

An LED emitting 464nm light (Doric Lenses Inc., Quebec, CAN) was positioned over area 17 of the visual cortex in order to activate ChR2 expressed in infected CG neurons. The LED cannula was embedded within the agar overlying the cortex and a shield was placed between the LED cannula and animals' eyes to prevent LED stimulation of retinal neurons. The manufacturer-stated maximum LED output is 5.5mW/mm^2, however we measured an average power output of ~2mW/mm^2 across experiments. Based upon previous measurements (1), we estimated the LED power to be near 100% at the center of the cannula, tapering off to around 10% (0.2mW/mm^2) at 2mm distant from the center of the cannula. Because layer 6 is 1-2mm beneath the cortical surface, we estimated the LED power in layer 6 to be a maximum of 1mW/mm^2 and a minimum of 0.2mW/mm^2 at the center of LED illumination and tapering off to negligible power >2mm from the center of surface illumination. We calculated the relative spatial spread and impact of the LED in receptive field coordinates by measuring the diameter of the LED spot and translating that into receptive field coordinates (degrees of visual space) according to a ferret area 17 magnification factor of 0.2mm/degree for eccentricities less than 20 degrees (5, 6). Following this calculation, the cone of LED illumination covered a spot with a radius of 5.2 visual degrees (**Fig. S2F**), which is roughly the size of a ferret parafoveal V1 receptive field (3, 4). Therefore, the spatial impact of the LED was on the order of a functional hyper-column.

The LED was flashed at the same temporal frequency as drifting gratings and phase-reversing gratings and was triggered at the onset of each grating cycle (corresponding to every other phase reversal for phase-reversing gratings). The duration of each LED flash was ~5ms (full width at half height). The LED was off in between stimulus presentations. The LED was on continuously during m-

sequence presentation. A separate LED-only stimulation protocol was used to measure neuronal responses to LED-only stimulation in the absence of visual stimulation. The monitor was either off or displayed mean grey during LED-only stimulation. For LED-only stimulation, the LED was flashed (~5ms duration per flash) for 2 seconds followed by 2 seconds of no activity. The frequency of LED flashes increased from 1-16Hz in 10 steps. LGN and V1 neuronal spiking and LFP responses to LED-only stimulation were measured. To quantify neuronal spiking responses to LED flashes of increasing frequency, similar to an LED "dose response curve", we calculated firing rate per trial (where LED flash rate varied per trial) for neurons in three subpopulations: 1) V1 LEDR neurons; 2) V1 non-LEDR neurons; and 3) LGN neurons. LED-only stimulation curves were then normalized by the spontaneous firing rate per neuron (**Figs. 1E**, **S2B**). To quantify the overall impact of LED-only stimulation on neurons in these different subpopulations, we measured the percent change in LED-only response magnitude, or the integral of the LED-only response curve (fit with smoothing splines), relative to spontaneous activity levels per neuron and averaged these values together across neurons in each subpopulation (**Fig. 1F**). Modulations of LGN and V1 neuronal populations by LED-only stimulation were assessed by examining LFP and CSD responses, as described above (see **Figs. 1D**, **S2G**).

For a subset of LGN neuronal recordings, we decoupled LED flash frequency from visual stimulus temporal frequency. We measured temporal frequency tuning responses in four conditions: 1) visual stimulus alone; 2) visual stimulus plus LED flashes at the frequency of the visual stimulus; 3) visual stimulus plus LED flashes fixed at 4Hz on all trials; and 4) visual stimulus plus LED flashes at twice the frequency of the visual stimulus. We calculated the firing rate at the preferred temporal frequency and the magnitude of the tuning response and compared these across the four conditions listed above. Results of this analysis are reported in Supplemental Results.

Analyses of visually evoked responses

Response curves for all well isolated LGN neurons were calculated from average firing rates in response to sinusoidal gratings varying in each measured parameter and were normalized to the peak in the corresponding without-LED condition. Curves were fit with power (contrast) or spline functions (spa-

20

tial and temporal frequency). Response metrics were obtained from curve fits of normalized responses and included: maximum firing rate (e.g. response rate to preferred stimuli), response magnitude (integral of curve fit relative to spontaneous rate), contrast to evoke a half-maximal response (c50), peak spatial and temporal frequencies, and the 50% high cut-off temporal frequency (TFhigh50) (**Fig. 5C**). LGN X and Y neurons were classified based on their responses to contrast and temporal frequency: Y neurons respond to lower contrast stimuli and follow higher temporal frequencies while X neurons prefer higher contrast stimuli and lower temporal frequencies (13). Our criteria for defining Y neurons was a c50 of <40% and a TFhigh50 of >15Hz. X neurons were defined with c50 >40% and TFhigh50 on the order of 15Hz or less.

Additional neuronal response properties were quantified for neurons recorded in experimental and control animals, including: spontaneous firing rate, maximum visually evoked firing rate, average visually evoked firing rate, and the rate of change of firing rate as the derivative of firing rate measured across 10ms windows. We calculated the hit rate for obtaining recordings from visually responsive LGN neurons in control and experimental animals as the number of recorded neurons with visually evoked tuning responses per penetration. The percentage of burst spikes among LGN neurons was obtained from grating and m-sequence data by identifying burst spikes as pairs of spikes with short inter-spike-intervals (less than 2ms) following a prior inter-spike-interval of at least 100ms.

Responses to m-sequence presentations were analyzed by calculating spike-triggered averages (STAs) of frames preceding each spike by a specified time. Fourth, third, second, and first frames preceding spikes were reverse-correlated, averaged, and compared across conditions with and without LED stimulation (see **Fig. 2**). LGN ON and OFF neurons were identified by receptive field brightness polarity in m-sequence STAs. The STA with the peak response (brightest light/dark pixels relative to background) was used to calculate a 2-dimensional Gaussian fit of the receptive field spatial profile. The width of the classical receptive field was calculated as the width of the ellipse containing pixels within 2 standard deviations of the mean pixel brightness of the Gaussian fit. Modulation of the STA over time (the temporal STA) was calculated as the brightness modulation across frames of the brightest pixels in the center of the receptive field in the peak STA frame. The temporal STA peak time was

the latency from the peak of the temporal STA curve fit (a Gaussian function) to the spike (at time zero; see **Figs. 2A** right, **2B**). The reduction in response latency was quantified as the difference in the time of the peak in the temporal STA (**Fig. 2A** right, arrowheads) across LED conditions and was calculated by subtracting the temporal STA peak time in the with LED condition from the temporal STA peak time in the without LED condition, such that negative values indicate the reduction in the temporal STA peak time with LED stimulation of CG feedback (see **Fig. 2C**). Variance in the temporal STA peak was calculated as the full-width at half height (FWHH) of the temporal STA peak in each LED condition (see **Figs. 2A**-**B**).

To measure spike-timing precision, spiking events were first determined from PSTHs of LGN and V1 neuronal responses to 20 repeats of phase-reversing sinusoidal gratings based on the timing of presentations of each stimulus phase in the without LED stimulation condition (see **Figs. 3A**-**B**). Spike timing precision was then calculated as the standard deviation of the first spike time in each event (14). To determine the visual onset response latency for each LGN and V1 neuron, the time to reach 50% of the maximum firing rate following the onset of a drifting sinusoidal grating was calculated from average PSTHs.

Statistical analysis

All data analyses were conducted using custom-written Matlab scripts. Almost all statistical comparisons involved comparing responses of the same sample of neurons across conditions with or without LED stimulation of CG feedback. These two-sample statistical comparisons were made using non-parametric t-tests following tests for distribution normality. Similarly, for comparisons of neuronal activity across experimental conditions (e.g. spontaneous firing rate in experimental versus control animals), two-sample non-parametric t-tests following tests for distribution normality were also used. Multiple sample non-parametric analysis of variance (ANOVA) tests were utilized for all comparisons with more than 2 samples, for example to compare percent change in response magnitude with LED-only stimulation for LEDR, non-LEDR, and LGN neurons (**Fig. 1F**).

SUPPLEMENTAL INFORMATION APPENDIX

Modeling LGN response latencies

In order to test whether a small change in CG firing rate could account for reductions in LGN onset response latencies observed in the data, we constructed a simple model of LGN responses and simulated LGN activity under conditions with and without LED stimulation of CG feedback. Note that the model simulation was oversimplified and did not take into account additional sources of input that could alter response rates and/or latencies such as arousal, attention, contrast, or adaptation. Code for the model was created using custom-written Matlab scripts. The response of an LGN relay neuron was modeled as a weighted sum of retinal, CG, and inhibitory inputs (**Fig. 4**) according to the following equation:

$$X_{LGN}(t) = W_{RGC} * X_{RGC}(t) + W_{CG} * X_{CG}(t) + W_{Inh} * X_{Inh}(t + tau)$$

where $X(t)$'s are PSTHs, W's represent weights, and tau is the disynaptic inhibition delay time. Latencies and time-courses for retinal and inhibitory PSTHs were adapted from the literature (15-17) and the CG PSTH was the average putative CG PSTH measured without LED stimulation. Weights and the disynaptic inhibition delay time (tau) were initially determined by fitting the modeled LGN response to the average LGN PSTH measured without LED stimulation of CG feedback (**Fig. 4B**, black curve) and minimizing the squared error in the fit using the 'fminsearch' function in Matlab. The following rules were imposed on the free parameters: $W_{RGC} > W_{CG}$; W_{RGC} and $W_{CG} > 0$; $W_{Inh} < 0$; and tau > 1ms. A second simulation was then run in which W_{RGC} was fixed according to the weight determined by the first simulation because the retinal input weight is not dependent upon changes in CG feedback. In the second simulation, the same rules were applied to the remaining free parameters and the modeled LGN response was fit to the average LGN PSTH measured with LED stimulation of CG feedback (**Fig. 4B**, blue curve) using the same methods. The CG input weights obtained from each simulation where then compared. As a control, a third simulation was performed in which all weights and tau were free parameters and the modeled LGN neuron was fit to the LGN PSTH measured with LED stimulation of CG feedback. The relative weights were similar and the CG input weight was increased by ~17%. However the error was higher for this simulation than the error for the second simulation in which the retinal input weight was fixed.

SUPPLEMENTAL INFORMATION APPENDIX

Histology

Following each recording session, animals were euthanized via injection of euthasol (200mg/kg, IP) and then perfused transcardially with phosphate buffered saline followed by 4% paraformaldehyde in phosphate buffer. Brains were extracted and placed in 20% sucrose in phosphate buffer. Blocks of brain including the LGN and visual cortex were frozen in sucrose and sectioned at 70μm thickness using a freezing microtome (Thermo Scientific, Waltham, MA). Sections were stained for cytochrome oxidase activity to visualize the cortical layers and the boundaries of subcortical structures. Sections were labeled first with a primary antibody against mCherry (rabbit anti-DS red, Clontech Labratories Inc., Mountain View, CA), followed by a biotinylated secondary antibody (goat anti-rabbit, Molecular Probes/Life Technologies, Grand Island, NY) before being reacted with DAB/peroxide to permanently label all neurons expressing mCherry. Sections were then mounted onto glass sides, defatted, and cover-slipped. Locations of electrode track lesions in V1 were observed such that proximity to optogenetically labeled CG neurons could be verified for all analyzed recording sessions (see **Fig. S1D**). Reconstructions of virus injection zone and LGN contours were made using a Neurolucida system (Micro-BrightField, Williston, VT) with an Optronics camera mounted to a microscope (Nikon Instruments Inc, Melville, NY). Virus-labeled LGN interneurons were marked in each reconstruction and manually counted. 3-d renderings of LGN volumes were made with Neurolucida software and volumetric data were extracted to measure relative volumes of virus injection zones relative to total LGN volumes (see **Fig. S1A**-**B**).

SUPPLEMENTAL INFORMATION APPENDIX

4. REFERENCES

1.   Huber D*, et al.* (2008) Sparse optical microstimulation in barrel cortex drives learned behavior in freely moving mice. *Nature* 451:61-64.
2.   Alitto HJ & Usrey WM (2004) Influence of contrast on orientation and temporal frequency tuning in ferret primary visual cortex. *J. Neurophys.* 91:2797-2808.
3.   Chapman B, Zahs KR, & Stryker MP (1991) Relation of cortical cell orientation selectivity to alignment of receptive fields of the geniculocortical afferents that arborize within a single orientation column in ferret visual cortex. *J. Neurosci* 11:1347-1358.
4.   Zahs KR & Stryker MP (1985) The projection of the visual field onto the lateral geniculate nucleus of the ferret. *J. Comparative Neurology* 241(2):210-224.
5.   Cantone G, Xiao J, McFarlane N, & Levitt JB (2005) Feedback connections to ferret striate cortex: direct evidence for visuotopic convergence of feedback inputs. *Journal of Comparative Neurology* 487(3):312-331.
6.   Law MI, Zahs KR, & Stryker MP (1988) Organization of primary visual cortex (area 17) in the ferret. *Journal of Comparative Neurology* 278(2):157-180.
7.   Sceniak MP, Hawken MJ, & Shapley R (2002) Contrast-dependent changes in spatial frequency tuning of macaque V1 neurons: effects of a changing receptive field size. *J. Neurophys.* 88:1363:1373.
8.   Osakada F*, et al.* (2011) New rabies virus varients for monitoring and manipulating activity and gene expression in defined neural circuits. *Neuron* 71:617-631.
9.   Wickersham IR, Finke S, Conzelmann KK, & Callaway EM (2007) Retrograde neuronal tracing with a deletion-mutant rabies virus. *Nature Methods* 4:47-49.
10.   Maier A, Adams GK, Aura C, & Leopold DA (2010) Distinct superficial and deep laminar domains of activity in the visual cortex during rest and stimulation. *Frontiers in Systems Neuroscience* 4:1-11.
11.   Kelly RC*, et al.* (2007) Comparison of recordings from microelectrode arrays and single electrodes in the visual cortex. *J. Neurosci* 27(2):261-264.
12.   Denman DJ & Contreras D (2015) Complex effects on in vivo visual responses by specific projections from mouse cortical layer 6 to dorsal lateral geniculate nucleus. *Journal of Neuroscience* 35(25):9265-9280.
13.   Sherman SM & Spear PD (1982) Organization of visual pathways in normal and visually deprived cats. *Physiological Reviews* 62(2):738-850.
14.   Berry MJ, Warland DK, & Meister M (1997) The structure and precision of retinal spike trains. *Procedings of the National Academy of Science USA* 94:5411-5416.
15.   McAlonan K, Cavanaugh JR, & Wurtz RH (2008) Guarding the gateway to cortex with attention in visual thalamus. *Nature* 456:391-394.
16.   Rathbun DL, Warland DK, & Usrey WM (2010) Spike timing and information transmission at retinogeniculate synapses. *Journal of Neuroscience* 30(41):13558-13566.
17.   Cafaro J & Rieke F (2013) Regulation of spatial selectivity by crossover inhibition. *Journal of Neuroscience* 33(15):6310-6320.